InsP_3-mediated intracellular calcium signalling is altered by expression of synaptojanin-1

Friedrich W. JOHENNING*†[1], Markus R. WENK‡[2], Per UHLÉN*, Brenda DEGRAY*, Eunkyung LEE‡[3], Pietro DE CAMILLI‡ and Barbara E. EHRLICH*[4]

*Departments of Pharmacology, Cell and Molecular Physiology, Yale University School of Medicine, New Haven, CT, U.S.A., †Institute for Anatomy, University Hospital Hamburg-Eppendorf, Hamburg, Germany, and ‡Departments of Cell Biology and Howard Hughes Medical Institute, Yale University School of Medicine, New Haven, CT, U.S.A.

Phosphatidylinositol 4,5-bisphosphate [PtdIns(4,5)P_2] plays an important physiological role as a precursor for the InsP_3-mediated intracellular calcium (Ca^{2+}) signalling cascade. It also regulates membrane trafficking, actin function and transmembrane proteins. SJ-1 (synaptojanin-1), a phosphoinositide phosphatase, regulates the turnover of a PtdIns(4,5)P_2 pool involved in clathrin and actin dynamics at the cell surface. We tested the interrelationship of this pool with PtdIns(4,5)P_2 pools involved in Ca^{2+} signalling by expressing in Chinese-hamster ovary cells full-length SJ-1 or its 5-Pase (inositol 5-phosphatase) domain. SJ-1 significantly attenuated the generation of Ca^{2+} oscillations induced by ATP and the 5-Pase domain mimicked this effect. These changes correlated with increased PtdIns(4,5)P_2 phosphatase activity of cellular extracts. Overexpression of the endoplasmic reticulum-anchored PtdIns(4)*P* phosphatase Sac1 did not affect Ca^{2+} oscillations, although it increased the Ca^{2+} efflux rate from intracellular stores. The ability of SJ-1 to alter intracellular Ca^{2+} signalling indicates a close functional interrelationship between plasma membrane PtdIns(4,5)P_2 pools that control actin and endocytosis and those involved in the regulation of specific spatio-temporal Ca^{2+} signals.

Key words: calcium signalling, calcium transient, fluorescent calcium dye, InsP_3, phosphoinositide phosphatase, synaptojanin-1.

INTRODUCTION

One major source of calcium (Ca^{2+}) is released from internal stores via InsP_3Rs (inositol 1,4,5-trisphosphate receptors) expressed on the membrane of the ER (endoplasmic reticulum). On ligand binding to heterotrimeric G-proteins or receptor tyrosine kinases, PLC (phospholipase C) becomes activated and cleaves the membrane-lipid PtdIns(4,5)P_2 (phosphatidylinositol 4,5-bisphosphate) into InsP_3 and diacylglycerol. InsP_3 then diffuses into the cytosol and activates the InsP_3R, which subsequently releases Ca^{2+} [1].

Changes in the intracellular free Ca^{2+} concentration determine a variety of distinct cellular functions. Examples are contraction in muscle cells, exocytosis in secretory cells, gene transcription or apoptosis. The Ca^{2+} ion encodes this diversity of information by differences in the spatial, temporal and quantitative nature of the increase in the intracellular free Ca^{2+} concentration [2]. On the level of the InsP_3R, this diversity can be generated by different biophysical properties of the InsP_3R subtypes I, II and III and their modulation by endogenous modulators such as associated proteins, protein kinase A and C phosphorylation, Ca^{2+} and ATP [3]. Increased sensitivity of InsP_3R activation can also be generated by the close proximity of the InsP_3R and InsP_3 generation in the subplasmalemmal space in regions now designated as Ca^{2+} signalling microdomains [4,5]. These interactions can determine the initiation of InsP_3R-induced Ca^{2+} signals and specificity of G-protein-coupled receptor signalling pathways. For example, a direct interaction between the InsP_3R and the lipid precursor of InsP_3, PtdIns(4,5)P_2, has been described in [6]. In single-channel measurements in planar lipid bilayers, PtdIns(4,5)P_2 serves as a tonic inhibitor of InsP_3R channel activity and InsP_3 binding to its receptor. This is the basis of a model where the association between PtdIns(4,5)P_2 and InsP_3R serves as an efficient coupling mechanism at sites of InsP_3 production although it remains to be seen whether in living cells PtdIns(4,5)P_2 (supposed to be primarily localized in the plasma membrane) can indeed interact with InsP_3R localized on intracellular membranes away from the plasma membrane [6].

PtdIns(4,5)P_2 has been to shown to inhibit and activate a wide range of different ion channels and transporters and to form signalling complexes with a wide range of cytoskeletal proteins and signalling molecules [7]. There is increasing evidence that PtdIns(4,5)P_2 functions as a direct effector in several cellular pathways in addition to providing InsP_3 on stimulation of PLC to hydrolyse PtdIns(4,5)P_2. Accordingly, PtdIns(4,5)P_2 degradation can also be achieved by phosphatases that dephosphorylate the inositol ring and do not allow subsequent generation of InsP_3. Furthermore, PtdIns(4,5)P_2 functions as the precursor for PtdIns(3,4,5)P_3, another important signalling lipid. As inositol metabolism plays major roles in membrane trafficking, cytoskeletal organization and signal transduction [8], the interaction among the PtdIns(4,5)P_2 pools that participate in these different cellular functions needs to be investigated.

Synaptojanin, a polyphosphoinositide phosphatase [9], is of particular interest because it metabolizes a variety of phosphoinositides including PtdIns(4,5)P_2. It contains two inositol phosphatase domains: a central inositol 5-phosphatase (5-Pase) domain can remove the 5′ phosphate of several phosphoinositides

Abbreviations used: CFP, cyan fluorescent protein; CHO, Chinese-hamster ovary; ER, endoplasmic reticulum; GFP, green fluorescent protein; InsP_3R, inositol 1,4,5-trisphosphate receptor; 5-Pase, inositol 5-phosphatase; PH, pleckstrin homology; PLC, phospholipase C; PtdIns(4,5)P_2, phosphatidylinositol 4,5-bisphosphate; SJ-1, synaptojanin-1.

[1] Present address: Physiologisches Institut, Ludwig-Maximillians Universität München, Pettenkoferstrasse 12, 80336 Munich, Germany.
[2] Present address: Department of Biochemistry, Faculty of Medicine, National University of Singapore, 8 Medical Drive, Singapore 117597, Singapore.
[3] Present address: Amgen, One Amgen Center Drive, Thousand Oaks, CA 91320-1799, U.S.A.
[4] To whom correspondence should be addressed (email barbara.ehrlich@yale.edu).

and inositol polyphosphates including PtdIns(4,5)P_2, PtdIns(3,4,5)P_3 and InsP_3 [10], and an N-terminal Sac1-like inositol phosphatase domain that can turn PtdIns(3)P, PtdIns(4)P and PtdIns(3,5)P_2 into PtdIns [11]. Synaptojanin also contains a C-terminal domain, which functions as a targeting domain. SJ-1 (synaptojanin 1) is the synaptojanin isoform most abundant in brain, where it is concentrated in nerve terminals. Its alternatively spliced targeting domain interacts with a variety of proteins implicated in clathrin-mediated endocytosis [9,12], the actin cytoskeleton and signal transduction [13].

Functional analysis of mice that had been modified to knockout expression of SJ-1 revealed a crucial role for this regulatory protein in synaptic vesicle recycling. The mice have neurological defects and die shortly after birth [14]. No connection between SJ-1 and Ca^{2+} signalling has been reported to date. The experiments described in the present study analyse the effects of heterologous expression of SJ-1 in CHO (Chinese-hamster ovary) cells and the resulting changes in PtdIns(4,5)P_2 content on ATP-mediated Ca^{2+} signalling. This non-neuronal cell type was chosen for these studies so that the effect of synaptojanin could be monitored in the absence of other synapse-specific proteins. We found that expression of synaptojanin or the 5-Pase domain significantly decreased intracellular Ca^{2+} signals induced by ATP. This demonstrates that SJ-1 may have direct effect on intracellular signalling independent of its role in membrane traffic and actin regulation.

MATERIALS AND METHODS

Plasmid construction

GFP-SJ-1 (where GFP stands for green fluorescent protein) and GFP-Sac1 constructs were generated by adding GFP from pEGFP-C1 (ClonTech) at the N-terminus of full-length human SJ-1 (P170) and rat Sac1 in pCDNA3 [15]. A GFP-phosphatase domain was generated by inserting the phosphatase domain of human SJ-1 (513–900 amino acids) into pEGFP-C1 using a pair of primers 5′ATTAAGCTTCTTCTAAAGTACTAAAGAGC (sense) and 5′AAAGGATCCGATTGAGACCAATACTGTACC (antisense). CFP-PLC-δ1(PH) (where CFP stands for cyan fluorescent protein and PH for pleckstrin homology) was generated as described previously [16].

Cell culture and transfection

CHO cells were grown in 90 % Dulbecco's modified Eagle's medium, a high glucose (4.5 g/l) medium supplemented with 10 % (v/v) foetal calf serum, 25 units/ml penicillin and 25 μg/ml streptomycin. Cells were grown to confluency in a water-saturated atmosphere at 37 °C and 5 % CO_2. For transfection, cells were eluted with Hanks balanced salt solution and plated on poly(L-lysine)-coated coverslips at a dilution of 1:40. After 24 h, cells were transfected using the indicated amounts of cDNA and LIPOFECTAMINE™ diluted in 1 ml of OPTIMEM for 210 min (2 μg of GFP and 6 μl of LIPOFECTAMINE™, 2 μg of SJ-1 and 6 μl of LIPOFECTAMINE™, 1 μg of 5-Pase and 6 μl of LIPOFECTAMINE™, 2 μg of Sac1 full-length and 4 μl of LIPOFECTAMINE™). Experiments were performed 24 h after transfection with GFP only, GFP-SJ-1 and CFP-PLC-δ1(PH) and 48 h after transfection with 5-Pase and Sac1.

CFP and GFP fluorescence measurements

Before Ca^{2+} imaging, expression levels of GFP constructs were measured using the Nikon PCM2000 confocal system. A 488 nm argon laser was used for GFP excitation, and a 515/30 nm band pass filter was used to collect GFP emission. All settings to measure GFP fluorescence were identical in experiments presented in Figures 3 and 4; these settings were chosen to optimize the measurement over the entire dynamic range of GFP expression levels and to minimize interference with Rhod-2. Settings for Rhod-2 measurements were generated from cells expressing GFP only, which were not loaded with Ca^{2+} indicators and which showed no bleed-through. Untransfected, but Rhod-2-loaded, cells were used to eliminate bleed-through when selecting settings to measure GFP. GFP intensity was measured in arbitrary units in regions of interests covering the cytoplasm.

CFP-PLC-δ1(PH)- and GFP-SJ-1-expressing cells were measured using a Zeiss LSM 510 META confocal microscope. The META detector records excitation lambda stacks that can be separated into individual cross-talk-free images corresponding to the signal from different dyes. A 458 nm argon laser was used for excitation and images were acquired by the META detector programmed to scan lambda stacks between 473 and 563 nm, in 10 nm steps. Using this procedure, doubly transfected cells could be determined. CFP images were collected in the interval 463–473 nm. To avoid CFP emission cross-talk, GFP-SJ-1-expressing cells were recorded using only the 488 nm argon laser and a 510/30 nm band pass filter. CFP intensity was measured in arbitrary units in regions of interest along the plasma membrane and covering the cytoplasm. The ratios between the CFP signal intensity along the plasma membrane and the cytoplasm were calculated and compared among cells expressing only CFP-PLC-δ1(PH) or both CFP-PLC-δ1(PH) and GFP-SJ-1. Values are presented as means $\pm$ S.E.M. for a minimum of eight cells.

Calcium imaging

To avoid interference from GFP labelling, the Ca^{2+}-sensitive dye Rhod-2 was used. Cells on glass coverslips were incubated in 1 μM Rhod-2 acetoxymethylester dissolved in 20 % Pluronic F127 and DMSO for 25 min followed by a 15 min de-esterification period. L15 medium was used as the extracellular solution for incubation and de-esterification. The coverslip was used as the bottom of an open superfusion chamber (Waner Instruments, Hamden, CT, U.S.A.). The chamber was mounted on to the stage of a Nikon E600 microscope with a 20×0.75 NA plain apochromat lens connected to a PCM 2000 confocal microscope.

Rhod-2 was excited with a 543 nm HeNe laser and emission was detected using a 585 nm long-pass filter. Optical sections of cells loaded with Rhod-2 were collected at 0.624 s/image. Rhod-2 measures both mitochondrial and cytosolic Ca^{2+}. Cytosolic Ca^{2+} signals were measured indirectly by monitoring the changes in nucleoplasmic Ca^{2+} concentrations in confocal sections < 1.5 μm. This approach minimized contributions from mitochondrial Ca^{2+} signalling. The correlation between nucleoplasmic Rhod-2 signals and cytosolic Ca^{2+} concentrations is validated in [25]. Increases in Ca^{2+} were measured as the ratio of fluorescence intensity of Rhod-2 over baseline (F/F_0). The self-ratio could underestimate the intranuclear-free Ca^{2+} concentration when large changes are measured. If the fluorescent signals are in the non-linear range of the dye, differences between the large and small Ca^{2+} transients might even be larger than reported previously [17]. Background fluorescence was subtracted from all experiments. There was no change in size, shape or location of the cells during the experiments.

The cells were perfused continually with Hepes-buffered saline at a rate of 2 ml/min. The chamber volume was 200 μl. Solution changes were accomplished rapidly by using a valve attached to a three-chambered superfusion reservoir. Cells were stimulated with 1 μM ATP between 30 and 90 s, followed by a 150 s washing

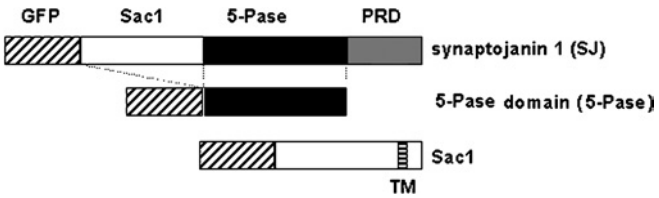

Figure 1 Constructs of SJ-1 used for the transfection

and a 1 min stimulation period with 10 μM ATP. All experiments were performed at 21 °C.

Data analysis

The baseline of the signal was defined as the average fluorescence measured before agonist application. A 5:1 running average filter was applied to all data sets. Cells were pooled in two groups depending on their GFP fluorescence intensity as determined directly before Ca^{2+} imaging (20–120 versus 121–255 arbitrary units).

For determining the fraction of cells responding at 1 μM ATP, only non-responding cells which showed a response at 10 μM ATP were included. A response was an increase in the F/F_0 ratio by > 10 % above baseline for longer than five consecutive frames (3.12 s). The flux rate was calculated as the slope of a line between the data point at which F/F_0 started to increase constantly above 25 % of the interval between F_0 and F_{peak} and the data point at which F/F_0 reached 75 % of the interval between F_0 and F_{peak}. Some cells showed appreciable responses but could not be included into the quantitative flux rate analysis due to baseline shifts. Differences are designated as significant if $P < 0.05$ using Student's t test; all values are displayed as means ± S.E.M.

Phosphoinositide phosphatase assay

CHO cells transfected with various GFP fusion proteins of phosphoinositide phosphatases were extracted by adding ice-cold buffer (30 mM Hepes, pH 7.4/100 mM KCl/1 mM EGTA/1 mM $MgCl_2$/1 % Triton X-100/0.5 ml per 10 cm culture dish) to the washed cell lawns and samples scraped and transferred to Eppendorf tubes. After 20 min incubation on ice, large debris was pelleted by brief centrifugation in a tabletop centrifuge. Supernatants were collected, adjusted for protein content and snap-frozen in liquid nitrogen. Aliquots (10 μl) were used in phosphatase assays using PtdIns(4,5)P_2 as a substrate [18]. Briefly, fluorescently [NBD (7-nitrobenz-2-oxa-1,3-diazole)] labelled PtdIns-(4,5)P_2 (1 μg; Echelon, Salt Lake City, UT, U.S.A.) was incubated with the cell extracts (20 μg of protein, $V = 50$ μl in buffer) for 20 min at 37 °C; the reaction products were extracted and separated as described in [19].

RESULTS

Expression of SJ-1 alters ATP-induced Ca^{2+} transients

Cells were transfected with the GFP-linked constructs of SJ-1 (Figure 1) as described in the Materials and methods section. Expression of GFP-SJ-1 resulted in a diffuse cytosolic fluorescence pattern, consistent with the absence of transmembrane regions in SJ-1 (Figure 2A). In CHO cells, ATP addition to the extracellular solution stimulates InsP_3 generation by activation of $P2Y_2$ receptors, which leads to Ca^{2+} release from intracellular stores. When transfected cells were stimulated with 1 and then 10 μM ATP for 120 s each, an increase in intracellular Ca^{2+}

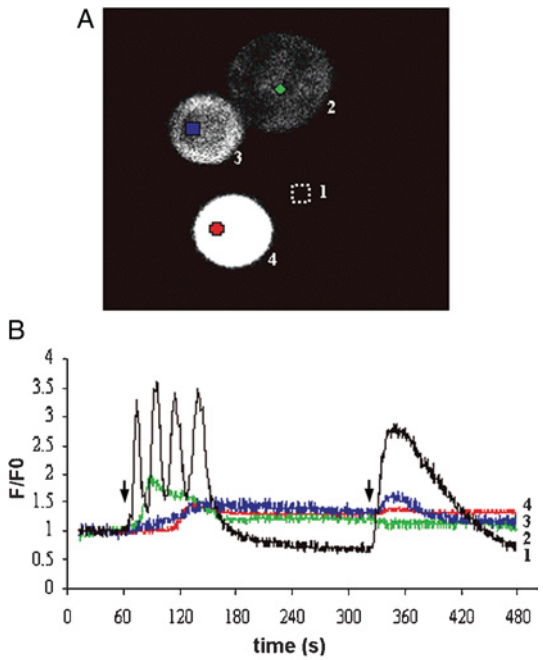

Figure 2 Expression levels of SJ-1 determine the magnitude, duration and latency of Ca^{2+} signalling in CHO cells

Expression levels of the GFP-SJ-1 fusion protein are shown in (**A**) and the corresponding time courses of changes in intracellular Ca^{2+} concentration are shown in (**B**); numbers in (**A**) correspond to numbered traces in (**B**). The black trace represents an untransfected control cell. Arrows on the time courses show when ATP stimulation occurred; at the first arrow 1 μM ATP and at the second arrow 10 μM ATP were added. ATP was applied for 120 s at each concentration.

concentration was observed (Figure 2B). In the range of ATP concentrations applied, the contribution of Ca^{2+} influx from the extracellular space is limited to the phase after the initial peak of the Ca^{2+} signal [20]. In Figure 2, the signal of the GFP-SJ-1-expressing cells on stimulation with 1 μM ATP for 120 s (red, blue and green traces) is attenuated and delayed in comparison with the untransfected control identified in the same visual field (black trace) [21]. Both the delay and the degree of attenuation correlate with the GFP-SJ-1 expression level determined by GFP fluorescence intensity (Figure 2A).

Effect of the 5-Pase domain of SJ-1 on ATP-induced Ca^{2+} transients

SJ-1 is a polyphosphoinositide phosphatase consisting of a central 5-Pase domain, an N-terminal Sac-like phosphatase domain and a proline-rich C-terminal sequence. The effect of full-length SJ-1 on intracellular Ca^{2+} transients was compared with the effect of the 5-Pase domain (Figures 3A and 3B). The response to 1 μM ATP depended on the expression levels of SJ-1. It was absent at high expression levels (Figure 3A, right panel, red trace) and reduced at lower expression levels (Figure 3A, right panel, green trace). This was also evident from the comparison with an untransfected control cell from the same experiment (Figure 3A, right panel, black trace). Expression of the 5-Pase abolished the response to 1 μM ATP (Figure 3B, right panel, blue and green traces) and reduced the response to 10 μM ATP depending on the expression level (Figure 3B, right panel, blue and green traces). The black trace refers to an untransfected cell from the same experiment and the red trace to a cell which does not respond to 10 μM ATP.

Control cells transfected with GFP only also exhibit a diffuse fluorescence pattern (Figure 3C, left panel). Note that in spite

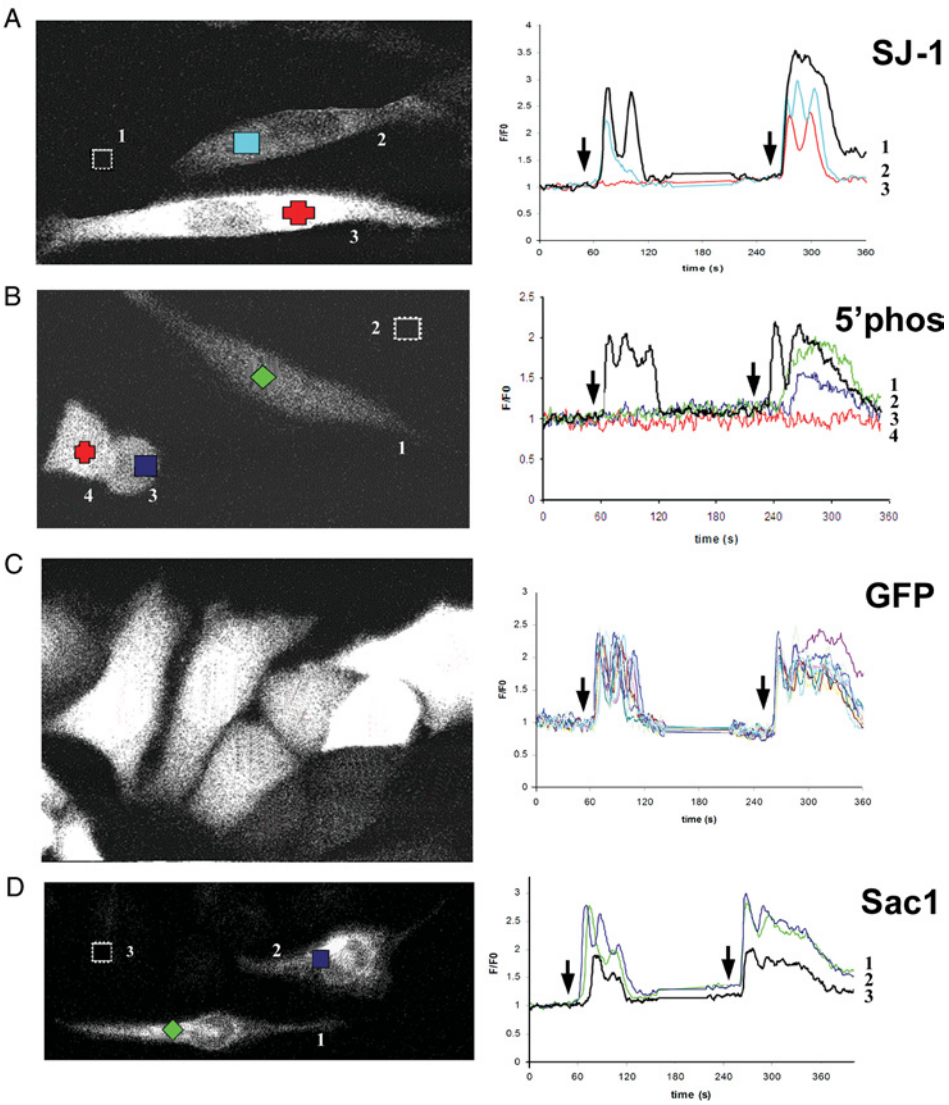

Figure 3 Expression of phosphoinositide phosphatases in CHO cells and the effect on intracellular Ca^{2+} signalling

Expression levels of the GFP fusion proteins indicated in Figure 1 are illustrated in the left-hand side panels of each pair. The magnitude of the expression was determined by the level of GFP expression. The coloured symbols in the left-hand side panels correspond to the traces in the right-hand side panels; the cells are also numbered to correspond to traces in the right-hand side panels. The traces in the right-hand side panels illustrate the time courses of changes in intracellular Ca^{2+} concentration. The black traces represent untransfected cells from the same experiment. Arrows on the time courses show when ATP stimulation occurred; at the first arrow 1 μM ATP and at the second arrow 10 μM ATP were added. ATP was applied for 120 s at each concentration.

of the large variation in GFP expression levels (Figure 3C, left panel), the amplitude, duration and slope of the rising phase of the ATP-stimulated signals were similar (Figure 3C, right panel). The GFP-only traces are similar to the internal controls from untransfected cells, which are displayed as black traces in the right panels of Figures 3(A), 3(B) and 3(D).

Expression of SJ-1 and 5-Pase diminishes the fraction of cells responding to ATP stimulation

To initiate a Ca^{2+} signal, the InsP_3 concentration must surpass an activation threshold. The next step was to determine whether changes in PtdIns(4,5)P_2 concentrations, which occurred as a consequence of SJ-1 or 5-Pase expression, could shift this threshold. For this purpose, only cells with a high level of GFP fluorescence, which served as an indicator of high protein expression levels, were included in the analysis. Cells which did not respond at the low concentration of ATP were only included in the analysis if they showed a response at 10 μM ATP to exclude effects from reduced cell viability.

Almost all control cells expressing GFP only (Figure 4, grey columns) responded at 1 μM ATP (97 % of the cells, $n = 41$), whereas for SJ-1 (Figure 4, black columns) a smaller fraction of cells responded (75 % of the cells, $n = 33$). When the 5-Pase domain of SJ-1 was expressed (Figure 4, white columns with grey diamonds), only 50 % of the cells displayed a Ca^{2+} transient ($n = 12$).

Ca^{2+} flux rate is decreased by SJ-1 and 5-Pase

The fraction of cells responding to submaximal stimulation is a qualitative indicator of changes in InsP_3-mediated Ca^{2+} signalling. This parameter predominantly reflects the probability of signal initiation. To quantify the changes induced by increased PtdIns(4,5)P_2 metabolism, the Ca^{2+} flux rate was measured as the slope of the initial rising phase of the signal. This parameter

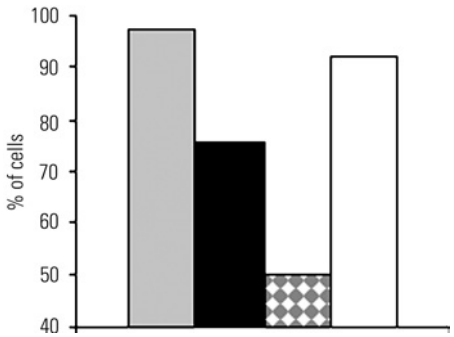

Figure 4 Fraction of CHO cells expressing phosphoinositide phosphatases responding to stimulation by 1 μM ATP

The fraction of cells with fluorescence intensity between 121 and 255 arbitrary units, designated as high expression, is displayed. Control cells expressing GFP only (grey column) at 1 μM ATP ($n = 17$) and 10 μM ATP ($n = 41$); SJ-1 (black column) at 1 μM ATP ($n = 33$) and 10 μM ATP ($n = 33$); 5-Pase domain (white column with grey diamonds) at 1 μM ATP ($n = 22$) and 10 μM ATP ($n = 12$); Sac1 (white column) at 1 μM ATP ($n = 57$) and 10 μM ATP ($n = 100$).

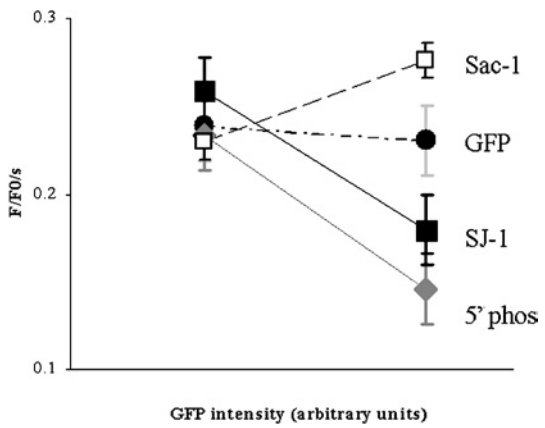

Figure 5 Ca^{2+} flux rates in CHO cells expressing phosphoinositide phosphatases as a function of protein expression

The fraction of cells with fluorescence intensity between 15 and 120 arbitrary units, designated as low expression, are displayed by the points on the left. The fraction of cells with fluorescence intensity between 121 and 255 arbitrary units, designated as high expression are displayed by the points on the right. With GFP expression only (●), there was no significant difference in the average Ca^{2+} flux rate of cells with high and low expression levels [0.24 ± 0.02/s ($n = 16$) versus 0.23 ± 0.02/s ($n = 41$)]. There was a decrease of the Ca^{2+} flux rate at high SJ-1 expression levels from 0.26 ± 0.02/s ($n = 24$) to 0.18 ± 0.02/s ($n = 25$). An even more pronounced decrease could be observed with 5-Pase expression from 0.23 ± 0.02/s ($n = 20$) to 0.13 ± 0.02/s ($n = 6$). When expressing full-length Sac1, there was a change from 0.23 ± 0.02/s ($n = 52$) to 0.28 ± 0.02/s ($n = 88$).

reflects the open probability of InsP_3R during the main activation phase, as defined by a net efflux of Ca^{2+} from the ER [22]. Cells were divided into two fractions with GFP fluorescence serving as an indicator of protein expression levels. The fraction of cells with a fluorescence intensity between 15 and 120 arbitrary units was designated as low expression (Figure 5, left bars) and the fraction of cells with a fluorescence intensity between 121 and 255 arbitrary units was designated as high expression (Figure 5, right bars). Identical settings were used for all the GFP measurements.

With GFP expression only, there was no significant difference in the average Ca^{2+} flux rate of cells with high and low expression levels [0.24 ± 0.02/s ($n = 16$) versus 0.23 ± 0.02/s ($n = 41$)]. There was a decline in the Ca^{2+} flux rate at high SJ-1 expression levels from 0.26 ± 0.02/s ($n = 24$) to 0.18 ± 0.02/s ($n = 25$). This was significant both in comparison with controls with high GFP expression only ($P = 0.02$) and when comparing high and low SJ-1 expression levels ($P = 0.003$) as an internal control. An even more pronounced decrease could be observed with 5-Pase expression, where the flux rate changed from 0.23 ± 0.02/s ($n = 20$) to 0.13 ± 0.02/s ($n = 6$). This was significant both in comparison with controls with high GFP expression only ($P = 0.03$) and when comparing high and low 5-Pase expression levels ($P = 0.04$).

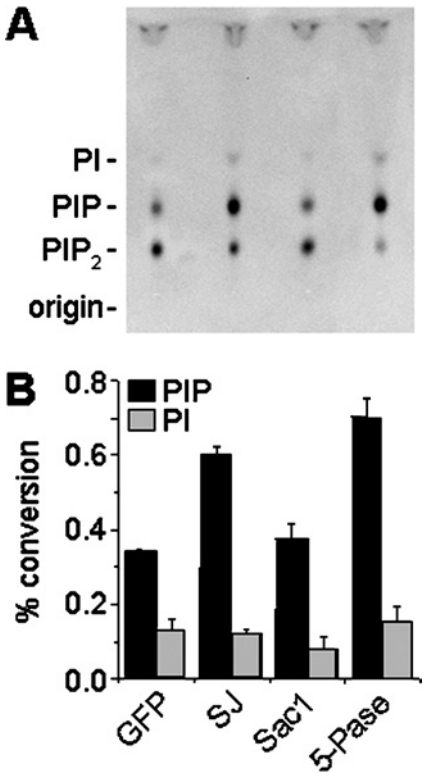

Figure 6 Phosphatase activities in CHO cells expressing phosphoinositide phosphatases

CHO cells were transfected with the fusion proteins as described in Figure 1. Cellular extracts were then assayed for phosphatase activity using PtdIns(4,5)P_2 as a substrate and reaction products separated by TLC (**A**). Overexpression of SJ-1 and its 5-Pase domain, but not GFP or Sac1, lead to increased degradation of PtdIns(4,5)P_2 to phosphatidylinositol phosphate (PIP), indicating an increased PtdIns(4,5)P_2 phosphatase activity in these cells (**B**). Levels of PtdIns (PI), the final dephosphorylation product of PtdIns(4,5)P_2, are not changed significantly among the samples. Results are represented as means $\pm$ S.D. ($n = 3$).

Increased PtdIns(4,5)P_2 phosphatase activity in cells expressing SJ-1 and its 5-Pase domain

Disruption of SJ-1 function leads to increased levels of PtdIns(4,5)P_2 in neurons, which result from a significantly reduced PtdIns(4,5)P_2 phosphatase activity of cytosolic extracts [14]. This indicates a major role of this enzyme in the metabolism of cellular PtdIns(4,5)P_2. We investigated whether overexpression of SJ-1 or 5-Pase leads, as expected, to the opposite effect, i.e. increased PtdIns(4,5)P_2 phosphatase activity. CHO cells were transfected with the fusion proteins as described in Figure 1 and protein extracts of the transfected cells were incubated with the substrate lipid, PtdIns(4,5)P_2. The reaction products were extracted and separated by TLC (Figure 6A). Under the assay conditions used, CHO cells expressing GFP only (control condition) converted approx. 30% of PtdIns(4,5)P_2 into phosphatidylinositol phosphate (Figure 6B). This effect was approx. double in cells expressing GFP-SJ-1 and its 5-Pase domain (Figure 6), indicating

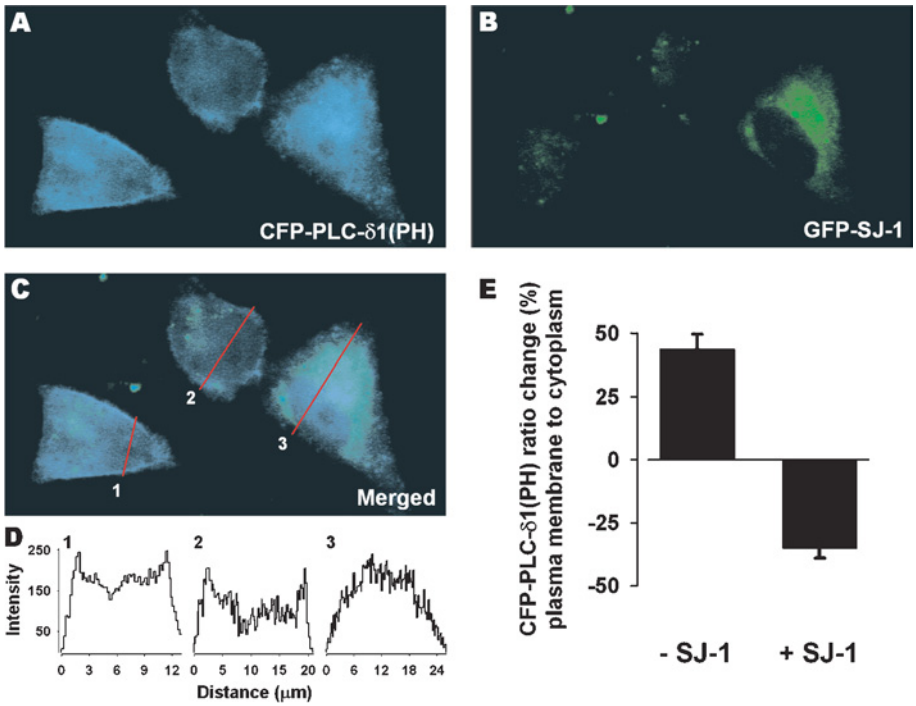

Figure 7 Plasma membrane expression of CFP-PLC-δ1(PH) in CHO cells

CFP-PLC-δ1(PH)-transfected cells (**A**) with one cell co-transfected with GFP-SJ-1 (**B**). The merged image of (**A**) and (**B**), shown in (**C**), reveals less membrane signal in the cell overexpressing GFP-SJ-1. (**D**) Cross-section intensity plot (indicated by red lines) of CFP-PLC-δ1(PH) distribution (**C**). (**E**) Ratio change of CFP-PLC-δ1(PH) emission intensity in percentage between regions along the plasma membrane and covering the cytoplasm in either non-transfected cells ($n = 14$) or GFP-SJ-1-transfected cells ($n = 8$). Results are represented as means ± S.E.M.

an overall increase in cellular PtdIns(4,5)P_2 phosphatase activity that should be reflected as reduced levels of PtdIns(4,5)P_2 *in vivo*.

Decreased PtdIns(4,5)P_2 levels at the plasma membrane in cells expressing SJ-1

To determine whether expression of SJ-1 altered the levels of PtdIns(4,5)P_2 in intact cells, the distribution of a fusion protein containing the PH domain of PLC-δ1 linked to CFP [CFP-PLC-δ1(PH)] was monitored in the presence and absence of GFP-linked SJ-1 (GFP-SJ-1). In cells containing only CFP-PLC-δ1(PH), there was intense staining along the plasma membrane, with a diffuse distribution inside the cell (Figure 7A). In contrast, in cells expressing GFP-SJ-1, the staining was predominantly in the interior of the cell and signal at the margins of the cell was faint (Figure 7B). When the magnitude of the CFP-PLC-δ1(PH) signal intensity was plotted along a cross-section through each cell, the cells expressing CFP-PLC-δ1(PH) alone have two peaks corresponding to the location of the plasma membrane, whereas the cells expressing both GFP-SJ-1 and CFP-PLC-δ1(PH) have the signal intensity shifted to the interior of the cell (Figure 7D). The ratio of the average signal at the plasma membrane and cell interior revealed a clear separation of the two types of expression (43.8 ± 5.9 % and -35.0 ± 4.0 %; Figure 7E), supporting the role of SJ-1 as a lipid phosphatase which will reduce the levels of PtdIns(4,5)P_2 *in vivo* at the plasma membrane.

Overexpression of the ER PtdIns(4)*P* phosphatase Sac1 does not affect Ca^{2+} transients, but increases the Ca^{2+} flux rate

As a further control, we also investigated cytosolic Ca^{2+} dynamics in cells overexpressing Sac1, a PtdIns(4)*P* phosphatase localized in the membrane of the ER. This protein, which contains a Sac1 domain homologous with the Sac1 domain of SJ-1, has similar enzymic properties with *in vitro* substrates which include PtdIns(3)*P*, PtdIns(4)*P* as well as PtdIns(3,5)P_2. Disruption of Sac1 in yeast cells primarily leads to an accumulation of PtdIns(4)*P*. The goal of these experiments was to determine whether phosphoinositide changes on the ER, where the InsP_3R is localized, could be involved in the observed effects. We expressed a GFP-Sac1 fusion protein, and the GFP fluorescence visible in these cells was strictly particulate, with an ER pattern, as expected (results not shown). GFP-Sac1 expressing cells showed an increase in the Ca^{2+} signal (Figure 3D, right panel, blue and green traces) when compared with the untransfected cell from the same experiment, at both 1 and 10 μM ATP (Figure 3D, right panel, black trace). Nearly all GFP-Sac1-transfected cells, similar to cells transfected with GFP alone, responded to 1 μM ATP. One interesting difference, however, consisting of a pronounced increase in the Ca^{2+} flux rate, was observed in cells with high levels of GFP-Sac1 expression. In the present study, a change from 0.23 ± 0.02/s ($n = 52$) to 0.28 ± 0.02/s ($n = 88$) was observed. This was significant both in comparing controls with high GFP expression only ($P = 0.04$) and when comparing high and low Sac1 expression levels ($P = 0.03$).

DISCUSSION

In the present study, we show that SJ-1 significantly attenuated ATP-mediated intracellular Ca^{2+} signalling in CHO cells. By using a non-neuronal cell type it was possible to determine the effect of synaptojanin in the absence of other synapse-specific proteins. The fraction of cells responding and the rate of Ca^{2+} release after stimulation by ATP decreased significantly. The 5-Pase domain of SJ-1 mimicked these effects on Ca^{2+} signalling. In contrast, Sac1, an ER-anchored PtdIns 4-phosphatase, increased the Ca^{2+} flux rate. This is consistent with the property of

the 5-Pase domain, but not of the SJ-1 Sac1 domain, to use PtdIns(4,5)P_2. When tested in biochemical assays, extracts of cells transfected with GFP-linked constructs of either SJ-1 or its 5-Pase domain revealed a significant increase in PtdIns(4,5)P_2 phosphatase activity. Similarly, the plasma membrane distribution of the PH domain of PLC-δ1, a marker for PtdIns(4,5)P_2 levels in intact cells, also was significantly decreased by the expression of SJ-1. These results demonstrate that the activities of phosphoinositide phosphatases are relevant for the regulation of intracellular Ca^{2+} signalling. The links between these enzymes and Ca^{2+} signalling raise important questions with respect to both the underlying molecular mechanism and the functional implications of these interrelations.

Extracellular application of ATP can mediate Ca^{2+} entry via three pathways: InsP_3 generation by activation of $P2Y_2$ receptors, opening of the $P2X_7$ receptor, which is a ligand-gated Ca^{2+} channel, or Ca^{2+} entry through store-operated channels which open on the plasma membrane in response to intracellular Ca^{2+} store depletion, often designated as capacitative Ca^{2+} entry. At the ATP concentrations applied (1 μM) in the experiments presented, only the PLC-coupled $P2Y_2$ receptor would be activated. Although the $P2X_7$ receptor is often co-expressed in CHO cells, this purinergic receptor has an EC_{50} in the range of 100 μM ATP [23]. Capacitative Ca^{2+} entry comes into play only after the initial peak of the Ca^{2+} signal, rather than as an initiator of the Ca^{2+} response. In addition, previous work on CHO cells shows that elimination of Ca^{2+} from the extracellular solution does not affect the rising phase to the peak of Ca^{2+} release but only the following components of the signal [20]. Consequently, the measured effects on Ca^{2+} flux rate and signal initiation must be due to InsP_3R-mediated Ca^{2+} signalling.

In this study, two aspects of the InsP_3R-mediated Ca^{2+} signal were analysed, the fraction of cells responding and the Ca^{2+} flux rate. The fraction of cells responding reflects the probability of generating a global InsP_3R-mediated Ca^{2+} transient. This feature is mainly altered by the fraction of InsP_3Rs involved in signal initiation, presumably those near the plasma membrane. The Ca^{2+} flux rate is a measure of the open probability of InsP_3R over the whole rising phase of the signal. This rate is an indicator of the fraction of the entire population of cytosolic InsP_3Rs activated throughout the entire rising phase of the signal [22]. It is important to note that the overexpression of SJ-1 attenuates both the initiation of InsP_3R-mediated Ca^{2+} signalling and the magnitude of the response once the signal has been initiated.

The molecular mechanism(s) used by SJ-1 to attenuate InsP_3R-mediated Ca^{2+} signalling remain(s) to be determined. SJ-1, via its 5-Pase domain, can use both PtdIns(4,5)P_2 and InsP_3 as substrates. Thus there are two basic mechanisms through which SJ-1 could interfere with InsP_3-mediated Ca^{2+} signalling. The most probable scenario is that SJ-1 may produce these effects by decreasing the steady-state level of PtdIns(4,5)P_2 in the plasma membrane. The reduction of PtdIns(4,5)P_2, in turn, would be responsible for a decreased production of InsP_3 on PLC activation. Alternatively, or in addition, increased SJ-1 could degrade InsP_3 more quickly, which would result in a slower increase in InsP_3 concentrations and a decreased steady-state level of InsP_3. In principle, full-length SJ-1, whose C-terminal domain interacts via components of plasma membrane-associated signalling scaffolds, should be more effective than the soluble 5-Pase in the degradation of PtdIns(4,5)P_2. Thus similar effects on Ca^{2+} signalling produced by overexpression of SJ-1 and of its 5-Pase domain raise the possibility that direct effects on InsP_3 levels may come into play. On the other hand, this lack of differential effect could be explained by the high level of overexpression of the two proteins.

The interactions between PtdIns(4,5)P_2 and InsP_3R-mediated Ca^{2+} signalling are complex. Three mechanisms that could account for the observed attenuation of InsP_3-mediated Ca^{2+} signalling by decreased steady-state PtdIns(4,5)P_2 levels are outlined here. The underlying assumption of the first hypothetical mechanism is that, after the activation of plasmalemmal G-proteins or receptor tyrosine kinases, PLC cleaves PtdIns(4,5)P_2 into InsP_3 and diacylglycerol. Reduction of PtdIns(4,5)P_2 simply reduces the substrate availability for the enzymic reaction generating InsP_3. SJ-1 and 5-Pase regulate Ca^{2+} signalling by indirectly modulating the rate of InsP_3 generation. The reduced substrate availability for InsP_3 generation explains both the impairment of signal initiation measured by reduction of the cells responding and the overall reduction in InsP_3R open probability reflected by slower Ca^{2+} flux rates.

The second potential mechanism is based on the function of PtdIns(4,5)P_2 as a lipid anchor, recruiting components of the Ca^{2+} signalling machinery. Plasma membrane PtdIns(4,5)P_2, in addition to functioning as a substrate for PLC, also recruits PLC via its binding to PH domains of PLCs. In addition, it may mediate a direct link with intracellular Ca^{2+} stores via an interaction 'in trans', with the InsP_3R. The proximity of the signalling molecules then increases the sensitivity of InsP_3R-mediated Ca^{2+} signalling. Reduction in steady-state PtdIns(4,5)P_2 by SJ-1 and 5-Pase would then result in the disruption of these complexes. The third possible mechanism relies on the role of PtdIns(4,5)P_2 as a second messenger where PtdIns(4,5)P_2 on its own generates increased sensitivity of Ca^{2+} signalling by activating 'in trans' InsP_3Rs. This interaction would also be decreased by overexpression of SJ-1 and 5-Pase. The second and third mechanisms rely on a close interaction between the InsP_3R and PtdIns(4,5)P_2 in the subplasmalemmal space. However, in our experiments, we have observed the Ca^{2+} transient over the nucleus to avoid signals from mitochondria. The Ca^{2+} flux rate measured in the nucleus is an excellent indicator of cytosolic InsP_3 concentrations and InsP_3R activity. It is unlikely that the small fraction of InsP_3R affected by direct interactions with PtdIns(4,5)P_2 on the plasma membrane has a major contribution once the signal is initiated. Therefore the last two mechanisms only explain the observed impairment of signal initiation measured by reduction of the cells responding. Direct interactions between PtdIns(4,5)P_2 and the InsP_3R cannot explain the overall reduction in InsP_3R open probability reflected by slower Ca^{2+} flux rates.

Results shown in the present study raise important questions, which go beyond the molecular mechanism of interaction between SJ-1 and Ca^{2+} signalling. They suggest a cross-talk between polyphosphoinositide phosphatases involved in vesicle trafficking and actin regulation and G-protein-coupled PLC cleavage of PtdIns(4,5)P_2 resulting in InsP_3R-mediated Ca^{2+} signalling. For example, SJ-1 knockout mice show severe neurological deficiencies and die shortly after birth [14]. The phenotype of SJ-1 knockout mice implies effects which have an impact on several aspects of signalling, not just on synaptic vesicle recycling. In SJ-1 knockout mice, Ca^{2+} release from internal stores would be amplified, where increases in Ca^{2+} release from internal stores tend to promote neurodegeneration (see [24] for a review). This hypothesis matches the observation that SJ-1 is up-regulated in cortical neurons of patients with Down's syndrome. Down's syndrome is associated with excessive neuronal loss and impairment of synaptogenesis. SJ-1 up-regulation in these patients might serve as a compensatory mechanism protecting neurons from excessive intracellular Ca^{2+} release [21].

The present study provides new insights into the interactions of plasmalemmal lipid metabolism and InsP_3-mediated Ca^{2+} signalling. Previously, only PLC cleavage of PtdIns(4,5)P_2 had been

connected with InsP_3-mediated Ca^{2+} signalling. There was no evidence of long-term effects of PLC activation on the plasmalemmal lipid composition affecting Ca^{2+} signalling. The connection between SJ-1, 5-Pase, Sac1 and InsP_3-mediated Ca^{2+} signalling provides a new principle where Ca^{2+} signalling can be regulated by long-term changes in the composition of plasma membrane lipid pools. 5-Pase, Sac1 or SJ-1 are constitutively active. They modulate the steady-state lipid content of the plasma membrane, thereby affecting the long-term activation threshold and sensitivity of InsP_3-mediated Ca^{2+} signalling. This effect can be spatially resolved. Signalling microdomains can be maintained by different subcellular expression patterns of phosphatases, which would result in spatially different compositions of lipid rafts. Clustered around signalling complexes, those rafts might affect differential Ca^{2+} signalling in distinct parts of a cell. Thus the expression pattern of constitutively active polyphosphoinositide phosphatases is a new mechanism determining subcellular differences in Ca^{2+} signalling.

This work was supported by grants from the NIH [GM63496 (B. E. E.), NS36251 (P. D. C.), CA46128 (P. D. C.) and DK54913 (P. D. C.)], Howard Hughes Medical Institute (P. D. C.) and Vetenskapsrådet, the Swedish Research Council (P. U.). F. W. J. was supported by a German National Merit Scholarship Foundation scholarship. We thank J. Barks (Nikon Instruments) for providing support and practical advice, and Nikon Instruments for the use of the Nikon E600 confocal microscope.

REFERENCES

1 Ehrlich, B. E., Kaftan, E., Bezprozvannaya, S. and Bezprozvanny, I. (1994) The pharmacology of intracellular Ca^{2+}-release channels. Trends Pharmacol. Sci. **15**, 145–149
2 Bootman, M. D. and Berridge, M. J. (1995) The elemental principles of calcium signaling. Cell (Cambridge, Mass.) **83**, 675–678
3 Thrower, E. C., Hagar, R. E. and Ehrlich, B. E. (2001) Regulation of Ins(1,4,5)P(3) receptor isoforms by endogenous modulators. Trends Pharmacol. Sci. **22**, 580–586
4 Delmas, P., Wanaverbecq, N., Abogadie, F. C., Mistry, M. and Brown, D. (2002) Signaling microdomains define the specificity and sensitivity of receptor-mediated InsP3 pathways in neurons. Neuron **34**, 209–220
5 Johenning, F. W. and Ehrlich, B. E. (2002) Signaling microdomains: InsP(3) receptor localization takes on new meaning. Neuron **34**, 173–175
6 Lupu, V. D., Kaznacheyeva, E., Krishna, U. M., Falck, J. R. and Bezprozvanny, I. (1998) Functional coupling of phosphatidylinositol 4,5-bisphosphate to inositol 1,4,5-trisphosphate receptor. J. Biol. Chem. **273**, 14067–14070
7 Hilgemann, D. W., Feng, S. and Nasuhoglu, C. (2001) The complex and intriguing lives of PIP2 with ion channels and transporters. Sci. STKE **2001**, RE19
8 Huijbregts, R. P., Topalof, L. and Bankaitis, V. A. (2000) Lipid metabolism and regulation of membrane trafficking. Traffic **1**, 195–202
9 McPherson, P. S., Garcia, E. P., Slepnev, V. I., David, C., Zhang, X., Grabs, D., Sossin, W. S., Bauerfeind, R., Nemoto, Y. and De Camilli, P. (1996) A presynaptic inositol-5-phosphatase. Nature (London) **379**, 353–357
10 Mitchell, C. A., Brown, S., Campbell, J. K., Munday, A. D. and Speed, C. J. (1996) Regulation of second messengers by the inositol polyphosphate 5-phosphatases. Biochem. Soc. Trans. **24**, 994–1000
11 Guo, S., Stolz, L. E., Lemrow, S. M. and York, J. D. (1999) SAC1-like domains of yeast SAC1, INP52, and INP53 and of human synaptojanin encode polyphosphoinositide phosphatases. J. Biol. Chem. **274**, 12990–12995
12 Ringstad, N., Nemoto, Y. and De Camilli, P. (1997) The SH3p4/Sh3p8/SH3p13 protein family: binding partners for synaptojanin and dynamin via a Grb2-like Src homology 3 domain. Proc. Natl. Acad. Sci. U.S.A. **94**, 8569–8574
13 Sakisaka, T., Itoh, T., Miura, K. and Takenawa, T. (1997) Phosphatidylinositol 4,5-bisphosphate phosphatase regulates the rearrangement of actin filaments. Mol. Cell. Biol. **17**, 3841–3849
14 Cremona, O., Di Paolo, G., Wenk, M. R., Luthi, A., Kim, W. T., Takei, K., Daniell, L., Nemoto, Y., Shears, S. B., Flavell, R. A. et al. (1999) Essential role of phosphoinositide metabolism in synaptic vesicle recycling. Cell (Cambridge, Mass.) **99**, 179–188
15 Nemoto, Y., Kearns, B. G., Wenk, M. R., Chen, H., Mori, K., Alb, Jr, J. G., De Camilli, P. and Bankaitis, V. A. (2000) Functional characterization of a mammalian Sac1 and mutants exhibiting substrate-specific defects in phosphoinositide phosphatase activity. J. Biol. Chem. **275**, 34293–34305
16 Sinnecker, D. and Schaefer, M. (2004) Real-time analysis of phospholipase C activity during different patterns of receptor-induced Ca^{2+} responses in HEK293 cells. Cell Calcium **35**, 29–38
17 Johenning, F. W., Zochowski, M., Conway, S. J., Holmes, A. B., Koulen, P. and Ehrlich, B. E. (2002) Distinct intracellular calcium transients in neurites and somata integrate neuronal signals. J. Neurosci. **22**, 5344–5353
18 Taylor, G. S. and Dixon, J. E. (2001) An assay for phosphoinositide phosphatases utilizing fluorescent substrates. Anal. Biochem. **295**, 122–126
19 Wenk, M. R., Pellegrini, L., Klenchin, V. A., Di Paolo, G., Chang, S., Daniell, L., Arioka, M., Martin, T. F. and De Camilli, P. (2001) PIP kinase Iγ is the major PI(4,5)P(2) synthesizing enzyme at the synapse. Neuron **32**, 79–88
20 Iredale, P. A. and Hill, S. J. (1993) Increases in intracellular calcium via activation of an endogenous P2-purinoceptor in cultured CHO-K1 cells. Br. J. Pharmacol. **110**, 1305–1310
21 Arai, Y., Ijuin, T., Takenawa, T., Becker, L. E. and Takashima, S. (2002) Excessive expression of synaptojanin in brains with Down syndrome. Brain Dev. **24**, 67–72
22 Ogden, D. and Capiod, T. (1997) Regulation of Ca^{2+} release by InsP3 in single guinea pig hepatocytes and rat Purkinje neurons. J. Gen. Physiol. **109**, 741–756
23 Kaznacheyeva, E., Zubov, A., Gusev, K., Bezprozvanny, I. and Mozhayeva, G. N. (2001) Activation of calcium entry in human carcinoma A431 cells by store depletion and phospholipase C-dependent mechanisms converge on ICRAC-like calcium channels. Proc. Natl. Acad. Sci. U.S.A. **98**, 148–153
24 Rizzuto, R. (2001) Intracellular Ca^{2+} pools in neuronal signalling. Curr. Opin. Neurobiol. **11**, 306–311
25 Collins, T. J., Lipp, P., Berridge, M. J. and Bootman, M. D. (2001) Mitochondrial Ca^{2+} uptake depends on the spatial and temporal profile of cytosolic Ca^{2+} signals. J. Biol. Chem. **276**, 26411–26420

Received 14 March 2004; accepted 14 April 2004
Published as BJ Immediate Publication 14 April 2004, DOI 10.1042/BJ20040418